Kinetics and Thermodynamics of Annexin A1 Binding to Solid-Supported Membranes: A QCM Study†

Katja Kastl,‡ Michaela Ross,§ Volker Gerke,|| and Claudia Steinem‡,*

Institut für Analytische Chemie, Chemo- und Biosensorik, Universität Regensburg, 93040 Regensburg, Germany, Institut für Biochemie, Westfälische Wilhelms-Universität, Wilhelm-Klemm-Strasse 2, 48149 Münster, Germany, and Institut für Medizinische Biochemie, Zentrum für Molekularbiologie der Entzündung (ZMBE), Westfälische Wilhelms-Universität, von-Esmarch-Strasse 56, 48149 Münster, Germany

Received April 12, 2002; Revised Manuscript Received June 12, 2002

ABSTRACT: By means of the quartz crystal microbalance (QCM) technique, the interaction of annexin A1 with lipid membranes was quantified using solid-supported bilayers immobilized on gold electrodes deposited on 5 MHz quartz plates. Solid-supported lipid bilayers were composed of a first octanethiol monolayer chemisorbed on gold and a physisorbed phospholipid monolayer obtained from vesicle fusion. This experimental setup enabled us to determine for the first time rate constants and affinity constants of annexin A1 binding to phosphatidylserine-containing layers as a function of the calcium ion concentration in solution and the cholesterol content within the outer leaflet of the solid-supported bilayer. The results reveal that a decrease in Ca^{2+} concentration from 1 mM to 100 μM significantly increases the rate of annexin A1 binding to the membrane independent of the cholesterol content. However, the presence of cholesterol in the membrane altered the affinity constants considerably. While the association constant decreases with decreasing Ca^{2+} concentration in the case of 1-palmitoyl-2-oleoyl-*sn*-glycero-3-phosphocholine (POPC)/1-palmitoyl-2-oleoyl-*sn*-glycero-3-phosphoserine (POPS) membranes lacking cholesterol, it remains high in the presence of cholesterol.

Ca^{2+} is one of the most prominent second messengers transmitting extracellular signals within the cell (*1*). The mechanisms of signal transduction triggered by calcium ions and the regulation of the intracellular calcium ion concentration are highly dynamic processes regulated by Ca^{2+} pumps, channels, and intracellular Ca^{2+}-binding proteins. Among them are the annexins, a family of cellular proteins that reversibly bind to cellular membranes in a Ca^{2+}-dependent manner (*2*−*4*). All annexins share a common structure composed of a conserved core and a variable N-terminal domain. The core typically comprises four or eight repeats of a 70-amino-acid sequence that harbor the calcium- and phospholipid-binding sites, while the variable N-terminal domain is thought to confer the specific properties of the annexin (*5*−*8*).

Annexin A1 has been shown to aggregate neutrophils and chromaffin cell granules as well as artificial membrane vesicles in a calcium-dependent fashion, suggesting that it might be involved in membrane trafficking (*9*−*13*). The first step in this process is the calcium-induced localization of annexin A1 to cellular membranes. X-ray crystallographic analysis (*7*, *14*−*16*) and mutagenesis studies (*17*−*21*) showed that the site responsible for the initial membrane binding of annexins to membranes (the primary membrane binding site) is located on one side of the annexin's core domain. Calcium ions bound to this side act as bridges connecting the protein with anionic lipid headgroups (*14*). The N-terminal domain, however, is involved in aggregating vesicles and is not specific for negatively charged lipids (*22*). Rosengarth et al. (*5*, *6*) were the first to solve the crystal structure of full-length annexin A1 containing the complete N-terminal domain in a calcium free environment. By controlled proteolysis with trypsin, de la Fuente et al. (*23*) demonstrated that annexin A1 undergoes a conformational change upon Ca^{2+}-dependent binding to lipid bilayers exposing a secondary lipid binding site. On the basis of these results, Rosengarth et al. (*6*) proposed a model in which the calcium-dependent binding of annexin A1 to negatively charged lipids induces the exposure of the N-terminal helical domain, which is thought to harbor the secondary phospholipid binding site.

The major objective of our study was to elucidate the kinetics and affinity constants of the calcium-ion-dependent binding of annexin A1 to phospholipid membranes. Most biochemical studies conducted so far have dealt with the determination of the Ca^{2+} concentration required for annexin A1 binding to phospholipid vesicles or cell membranes using vesicle assays (*2*, *24*−*26*). To our knowledge, association constants of annexin A1 binding to phospholipids at a constant calcium ion concentration in solution have not been determined yet, and no data are available describing the kinetics of annexin A1 interaction with lipid membranes. Since the function of annexin A1 is predominately determined by its dynamic behavior upon a calcium ion trigger

† This is a contribution from the Graduate College 760

* To whom correspondence should be addressed. Telephone: +49 941 943 4548. Fax +49 941 943 4491. E-mail: claudia.steinem@chemie.uni-regensburg.de.

‡ Institut für Analytische Chemie, Chemo- und Biosensorik, Universität Regensburg.

§ Institut für Biochemie, Westfälische Wilhelms-Universität Münster.

|| ZMBE, Westfälische Wilhelms-Universität Münster.

10.1021/bi025951z CCC: $22.00
Published on Web 07/12/2002

in the cell, the kinetics of protein binding are an important parameter. For a quantitative and detailed kinetic and thermodynamic analysis of annexin A1 membrane binding, solid-supported lipid bilayers are well suited since only protein adsorption to one distinct membrane is measured. Moreover, interference from membrane aggregation due to the secondary membrane binding site of annexin A1, which is exposed following the primary, Ca^{2+}-dependent binding, is avoided by using solid-supported lipid bilayers.

To study lipid−protein interactions on solid supports, several common techniques are available including optical (ellipsometry, surface plasmon resonance spectroscopy, interferometry) and electrochemical methods (cyclovoltammetry, impedance spectroscopy). Besides these well-established techniques, the quartz crystal microbalance (QCM)[1] has also been recognized in recent years as a versatile and label-free technique to follow adsorption processes at solid/liquid interfaces in chemical and biological research (*27*, *28*). In combination with solid-supported lipid membranes, the quartz crystal microbalance technique allows the elucidation of thermodynamic and kinetic parameters of protein−ligand pairs in a label-free fashion due to the correspondence of frequency change to adsorbed mass (*29*).

MATERIALS AND METHODS

Materials. The phospholipids 1-palmitoyl-2-oleoyl-*sn*-glycero-3-phosphocholine (POPC) and 1-palmitoyl-2-oleoyl-*sn*-glycero-3-phosphoserine (POPS) were purchased from Avanti Polar Lipids (Alabaster, AL). Cholesterol, Tris, and EGTA were obtained from Sigma (Deisenhofen, Germany), and octanethiol was from Fluka (Neu Ulm, Germany). NaN_3, $CaCl_2$, NaCl, and HCl were purchased from Merck (Darmstadt, Germany). The gold used for the working electrodes was a friendly gift from DEGUSSA (Hanau, Germany). The chromium was from Bal Tec (Balzers, Liechtenstein). All chemicals were of highest purity available. The 5 MHz overtone polished AT-cut quartz crystals (plano-plano) were from KVG (Neckarbischofsheim, Germany). Water was purified first through a Millipore water purification system Milli Q RO 10 Plus and then finally with the Millipore ultrapure water system Milli Q Plus 185 (specific resistance: 18.2 MΩ/cm).

Protein Purification. Full-length recombinant porcine annexin A1 was purified according to Rosengarth et al. (*30*). Protein concentration was determined by UV absorption with $\epsilon_{280} = 0.6$ cm^2 mg^{-1}, and protein purity was analyzed by SDS PAGE.

Vesicle Preparation. Mixed lipid films were prepared by drying the lipids dissolved in chloroform under a stream of nitrogen followed by 2 h under vacuum at 40 °C and stored at 4 °C. Multilamellar vesicles (MLVs) were prepared by first swelling the lipid films in buffer solution (20 mM Tris/HCl, 0.1 M NaCl, 1 mM EGTA, 1 mM NaN_3, pH 7.4), followed by periodically vortexing them for 30 s every 5 min. The resulting MLVs were subsequently converted into large unilamellar vesicles (LUVs) by pressing the MLVs through a polycarbonate membrane (100 nm pore diameters) using a miniextruder (Liposo Fast, Avestin).

Preparation of Lipid Bilayers on Gold. The gold electrodes were first cleaned in an argon plasma for 5−10 min (Plasma Cleaner, Harrick, NY) before placing the quartz plate in the Teflon cell and incubating the surface in a 1 mM solution of octanethiol in ethanol for 1 h. Subsequently, the gold surface was rinsed several times with ethanol in order to remove remaining thiols and then with a buffer solution consisting of 20 mM Tris/HCl, 0.1 M NaCl, 1 mM EGTA, 1 mM NaN_3, pH 7.4 to remove ethanol. The completeness of chemisorption was checked by impedance spectroscopy. Chemisorption was called successful when the determined capacitance was 2.0 ± 0.2 μF/cm^2.

The second monolayer was composed of 1-palmitoyl-2-oleoyl-*sn*-glycero-3-phosphocholine (POPC) and 1-palmitoyl-2-oleoyl-*sn*-glycero-3-phosphoserine (POPS) in a molar ratio of 4:1 with or without 30 mol % cholesterol. The lipid monolayer was achieved by adding the preformed LUVs to the hydrophobic octanethiol monolayer and incubating for 1 h at room temperature to induce fusion of the vesicles on the hydrophobic monolayer (*31*). The quality of the solid-supported bilayer was again checked by impedance spectroscopy. A successful preparation results in capacitance values of 1.1 ± 0.2 μF/cm^2. Remaining vesicles were removed by exchanging the vesicle suspension against pure buffer. Prior to the QCM measurements, the buffer solution was exchanged against buffer solution containing varying $CaCl_2$ concentrations.

Impedance Analysis. The solution exposed gold electrode with an area of 0.3 cm^2 evaporated on a 5 MHz quartz plate served as working electrode, and a platinized platinum wire was used as counter electrode. A.c. impedance analysis was performed with an impedance gain/phase analyzer from Solartron Instruments (Farnborough, U.K.). Impedance spectra ($|Z(f)|$, $\Phi(f)$) were recorded in a frequency range of 10^{-1}−10^6 Hz with an a.c. amplitude of 30 mV (rms).

QCM Measurements. The experimental setup for the QCM measurements used in the present study is shown in Figure 1. AT-cut quartz plates (14 mm in diameter) with a 5 MHz fundamental resonance frequency were coated with gold electrodes (0.3 cm^2) on both sides, mediated to the quartz plate by a thin chromium layer. The quartz plate was placed in a fluid chamber made of Teflon, exposing one side of the resonator to the aqueous solution. Equipped with an inlet and outlet connecting the fluid chamber to a peristaltic pump, the setup allows adding protein solution from outside the Teflon chamber. Spring contacts connected the gold electrodes of the quartz plate with the oscillator circuit (TTL SN74LS124N, Texas Instruments, Dallas, TX) located underneath the Teflon chamber. The entire system was placed in a water-jacketed Faraday cage thermostated at 20 °C. The frequency change of the quartz resonator was recorded using a frequency counter (HP 53181A, Hewlett-Packard, San Diego, CA) connected via RS 232 to a personal computer. The oscillator circuit was supplied with a voltage of 4 V by a d.c. power supply (HP E3630A, Hewlett-Packard, San Diego, CA).

To investigate the reversibility of annexin A1 binding to membranes, we used EGTA to complex calcium ions after

[1] Abbreviations: QCM, quartz crystal microbalance; POPC, 1-palmitoyl-2-oleoyl-*sn*-glycero-3-phosphocholine; POPS, 1-palmitoyl-2-oleoyl-*sn*-glycero-3-phosphoserine; SDS, sodium dodecyl sulfate; PAGE, polyacrylamide gel electrophoresis; EGTA, ethylene glycol bis(β-aminoethyl ether)-*N*,*N*,*N*′,*N*′-tetraacetic acid; MLV, multilamellar vesicle; LUV, large unilamellar vesicle; MDCK, Madine-Darby canine kidney; POPE, 1-palmitoyl-2-oleoyl-*sn*-glycero-3-phosphoethanolamine; PS, phosphatidylserine; PC phosphatidylcholine.

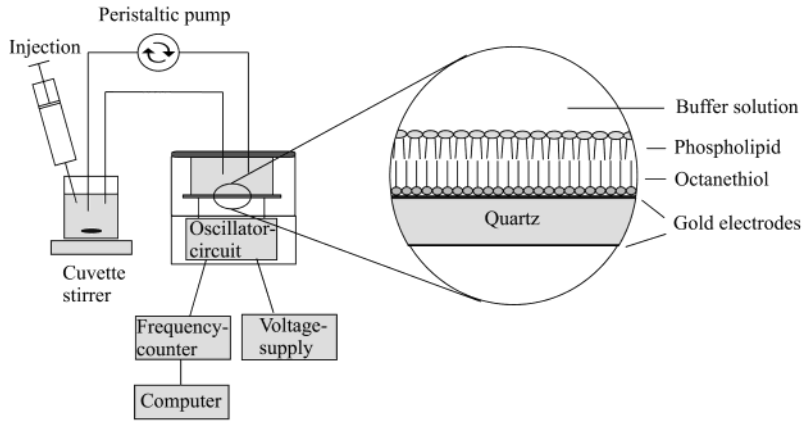

FIGURE 1: Experimental setup of the quartz crystal microbalance to monitor protein adsorption in a time-resolved fashion. The protein solution is injected into a small vessel and then added via a peristaltic pump to the quartz crystal, while the resonance frequency of the quartz plate is read out continuously by a frequency counter.

complete adsorption of the protein in the presence of Ca^{2+}. After adding protein solution, different amounts of EGTA solutions (20 mM Tris/HCl, 0.1 M NaCl, 1 mM NaN_3, pH 7.4 with either 10, 50, or 100 mM EGTA) were injected. Free calcium ion concentrations were calculated according to Stockbridge (*32*) using a program written in *Mathcad 2001*.

RESULTS

Interaction of Annexin A1 with Solid-Supported Membranes. Solid-supported membranes composed of an octanethiol monolayer and a second phospholipid monolayer immobilized on 5 MHz quartz plates have been proven to be well-suited for the investigation of lipid−protein interactions (*29*, *33*−*35*). Here, we applied this system to investigate the interaction of full-length annexin A1 with lipid layers. At first, quartz crystal microbalance (QCM) experiments were performed using POPC/POPS (4:1) lipid layers. Prior to the QCM experiment, the electrical parameters of each octanethiol monolayer and lipid bilayer were determined routinely by means of impedance analysis to ensure a surface coverage larger than 95%, which is a prerequisite for reproducible QCM measurements. Impedance spectra were modeled using an equivalent circuit composed of a capacitance C_m representing the octanethiol monolayer and the lipid bilayer, respectively, in series to an Ohmic resistance R_e representing the bulk resistance and the wire connections. This equivalent circuit is valid as octanethiol monolayers, and the corresponding lipid bilayers are almost defect-free, leading to a sole capacitive behavior in the observed frequency regime (*36*). By fitting the equivalent circuit to the data, the capacitance of the octanethiol monolayer was determined to be 2.0 ± 0.2 μF/cm^2. For lipid bilayers, composed of an octanethiol monolayer and a second POPC/POPS monolayer (see Figure 1), a mean capacitance value of 1.1 ± 0.2 μF/cm^2 was obtained. Assuming a series connection of the capacitances of the two monolayers allows calculating the specific capacitance of the second phospholipid monolayer, which was determined to be 2.4 ± 0.6 μF/cm^2.

The lipid bilayers prepared and characterized as described were used for studying annexin A1 binding by means of the quartz crystal microbalance technique. Figure 2 shows a typical time course of the frequency shift of the quartz plate upon addition of three different annexin A1 concentrations to a POPC/POPS (4:1) membrane in the presence of 1 mM $CaCl_2$. At a constant resonance frequency, protein solution was injected into the cup, and the resonance frequency was monitored. Adsorption of annexin A1 to the solid-supported lipid bilayer is revealed by the decrease in resonance frequency. Δf is defined as the difference between the actual resonance frequency $f(t)$ and $f(t = 0)$. Similar experiments were performed using pure POPC membranes lacking negatively charged POPS. In this case, addition of protein up to a concentration of 0.4 μM in the presence of 1 mM $CaCl_2$ did not alter the resonance frequency of the quartz plate. Thus, under the conditions chosen, annexin A1 adsorbs specifically to negatively charged POPS.

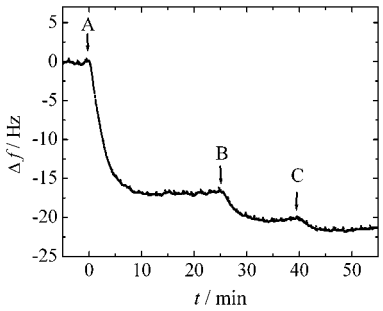

FIGURE 2: Typical time-dependent frequency trace revealing annexin A1 adsorption to solid-supported membranes, composed of an octanethiol monolayer chemisorbed on gold, and a POPC/POPS (4:1) monolayer in 20 mM Tris/HCl, 0.1 M NaCl, 1 mM NaN_3, 1 mM $CaCl_2$, pH 7.4. The arrows indicate the time when protein solution was injected (A, 0.27 μM; B, 0.53 μM; C, 0.78 μM annexin A1). The values at equilibrium after protein addition are $\Delta f_e = -16.8 \pm 0.5$ (A), -20.5 ± 1.0 (B), and -21.5 ± 1.5 (C) Hz.

Association Constants and Kinetics of Annexin A1 Binding to POPC/POPS Membranes. For a quantitative analysis of the kinetics of protein binding, we assumed that the rate-limiting step is the adsorption of the protein on the surface and that all individual protein binding sites are independent of each other, i.e. noncooperative. A rate-limited kinetics can then be ascribed by eq 1:

$$\Delta f(t) = \Delta f_e(1 - \exp(-k_s t)) \quad (1)$$

where Δf_e is the equilibrium frequency shift for a given protein concentration c_{AnxA1} in solution and k_s the protein

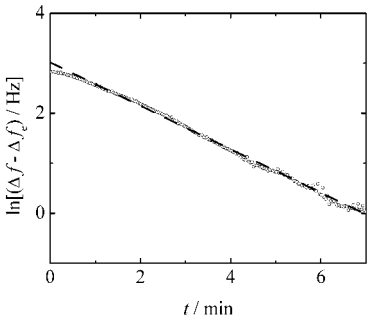

FIGURE 3: Linearization of the time-dependent frequency trace (0−7 min) shown in Figure 2 according to eq 2. The annexin A1 concentration in the bulk solution was 0.27 μM. The broken line is the result of fitting the parameter of eq 2 to the data. k_s was determined to be 6.7 ± 0.2 ms^{-1}.

concentration-dependent rate constant. By linearizing eq 1 (eq 2):

$$\ln(\Delta f(t) - \Delta f_e) = \ln(\Delta f_e) - k_s t \quad (2)$$

we can obtain the rate constant k_s for a given protein concentration in the bulk phase. Linearization allowed us to readily visualize deviations from a monoexponential behavior. A result of such a fitting procedure is depicted in Figure 3 as a broken line.

By performing concentration-dependent measurements, we can obtain affinity constants and rate constants of association and dissociation. According to Sauerbrey (*37*), it is assumed that the frequency shift is proportional to the adsorbed mass. Hence, adsorption isotherms can be obtained from measuring Δf_e for various annexin A1 concentrations. A theoretical model, which is also the simplest one to describe an adsorption isotherm, is given by Langmuir (eq 3):

$$\Delta f_e(c_{AnxA1}) = \Delta f_{max} \frac{c_{AnxA1} K_{ass}}{1 + c_{AnxA1} K_{ass}} \quad (3)$$

Δf_{max} is the frequency shift at maximum surface coverage and K_{ass} the association constant of annexin A1 binding to the phospholipid layer. Rate constants of association k^+ and dissociation k^- can be derived according to eq 4 from concentration-dependent measurements of the rate constant k_s:

$$k_s(c_{AnxA1}) = k^+ c_{AnxA1} + k^- \quad (4)$$

Figure 4 shows adsorption isotherms of annexin A1 binding to POPC/POPS (4:1) as a function of calcium ion concentration in solution. As a control, annexin A1 was added to POPC/POPS layers in the absence of calcium ions in the bulk phase up to protein concentrations of 0.25 μM. In this case, no frequency shift was detected upon protein addition indicating that annexin A1 adsorption to these membranes at pH 7.4 does not occur in a calcium ion independent fashion. Calcium-ion-dependent measurements were carried out in 20 mM Tris/HCl, 100 mM NaCl, 1 mM NaN_3 at pH 7.4 containing 100 μM or 1 mM $CaCl_2$. Fitting the parameters of eq 3 to the data shown in Figure 4 leads to a maximum frequency shift of $\Delta f_{max} = -21 \pm 1$ Hz and a corresponding association constant of $K_{ass} = 1.7 \pm 0.2 \times 10^7$ M^{-1} in 1 mM $CaCl_2$ solution. A decrease in $CaCl_2$ concentration to 100 μM does not influence the maximum frequency shift considerably, which was determined to be $\Delta f_{max} = -17 \pm 2$ Hz, while the association constant is decreased by a factor of 4 to $K_{ass} = 3.8 \pm 0.7 \times 10^6$ M^{-1}. In Figure 5, k_s as a function of annexin A1 concentration in the bulk phase is plotted for 1 mM and 100 μM $CaCl_2$ in solution. k^+ and k^- were obtained from fitting the parameters of eq 4 to the data. In the presence of 1 mM $CaCl_2$, the rate constant of association was determined to be $k^+ = 1.4 \pm 0.3 \times 10^4$ M^{-1} s^{-1}, while the one for dissociation is $k^- = 3 \pm 1 \times 10^{-3}$ s^{-1}. At a calcium ion concentration of 100 μM, a rate constant of association of $k^+ = 5.3 \pm 0.6 \times 10^4$ M^{-1} s^{-1} is obtained, being approx. a factor of 4 larger than in the presence of 1 mM $CaCl_2$, while the rate constant of dissociation with a value of $k^- = 7.0 \pm 1.5 \times 10^{-3}$ s^{-1} is approx. two times larger.

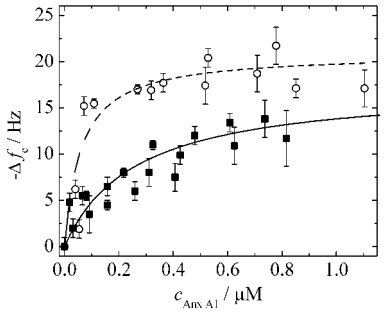

FIGURE 4: Langmuir adsorption isotherms of annexin A1 to POPC/POPS (4:1) layers in 20 mM Tris/HCl, 0.1 M NaCl, 1 mM NaN_3, 1 mM $CaCl_2$ (open circles) and 100 μM $CaCl_2$ (filled squares) at pH 7.4. The dotted line represents the result of fitting the parameters of eq 3 to the data for 1 mM $CaCl_2$. The values of the parameters are $\Delta f_{max} = -21 \pm 1$ Hz and $K_{ass} = 1.7 \pm 0.2 \times 10^7$ M^{-1}. Using 100 μM $CaCl_2$, the fitting procedure leads to the solid line with the parameters $\Delta f_{max} = -17 \pm 2$ Hz and $K_{ass} = 3.8 \pm 0.7 \times 10^6$ M^{-1}.

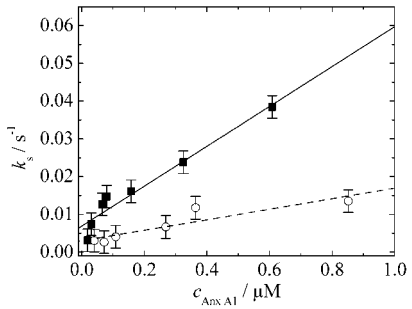

FIGURE 5: Rate constants of protein adsorption to POPC/POPS (4:1) membranes as a function of the annexin A1 concentration in 20 mM Tris/HCl, 0.1 M NaCl, 1 mM NaN_3, 1 mM $CaCl_2$ (open circles) and 100 μM $CaCl_2$ (filled squares) at pH 7.4. The dotted line is the result of fitting the parameters of eq 4 to the data for 1 mM $CaCl_2$. The values are $k^+ = 1.4 \pm 0.3 \times 10^4$ M^{-1} s^{-1} and $k^- = 3 \pm 1 \times 10^{-3}$ s^{-1}. In the presence of 100 μM $CaCl_2$, the linear regression results in the solid line with the parameters $k^+ = 5.3 \pm 0.6 \times 10^4$ M^{-1} s^{-1} and $k^- = 7.0 \pm 1.5 \times 10^{-3}$ s^{-1}.

Association Constants and Kinetics of Annexin A1 Binding to POPC/POPS/Cholesterol Membranes. Cholesterol is a major component of the plasma membrane of all animal cells, and it has been implicated in the membrane binding of some annexins (for review, see ref *4*). Therefore, we next analyzed whether cholesterol affects the adsorption of annexin A1 to negatively charged phospholipids. A cholesterol content of 30 mol % was added to the POPC/POPS (4:1) lipid mixture, which is a typical amount found in biological membranes.

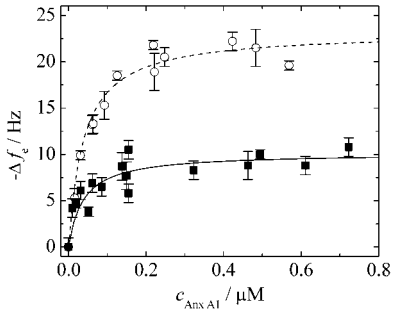

FIGURE 6: Langmuir adsorption isotherms of annexin A1 to POPC/POPS/cholesterol bilayers (56:14:30) in 20 mM Tris/HCl, 0.1 M NaCl, 1 mM NaN_3, 1 mM $CaCl_2$ (open circles) and 100 μM $CaCl_2$ (filled squares) at pH 7.4 The dotted line illustrates the result of fitting the parameters of eq 3 to the data for 1 mM $CaCl_2$. The values of the parameters are $\Delta f_{max} = -23 \pm 1$ Hz and $K_{ass} = 2.6 \pm 0.2 \times 10^7$ M^{-1}. For 100 μM $CaCl_2$ (solid line), $\Delta f_{max} = -10 \pm 1$ Hz and $K_{ass} = 2.6 \pm 0.4 \times 10^7$ M^{-1} were obtained.

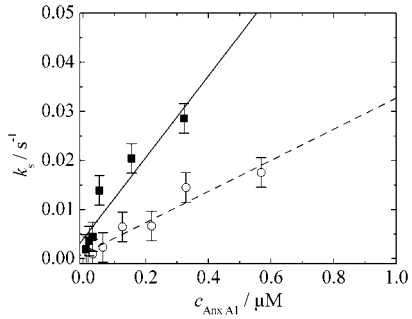

FIGURE 7: Rate constants of protein adsorption to POPC/POPS/cholesterol (56:14:30)-membranes dependent on the concentration of annexin A1 in 20 mM Tris/HCl, 0.1 M NaCl, 1 mM NaN_3, 1 mM $CaCl_2$ (open circles) and 100 μM $CaCl_2$ (filled squares) at pH 7.4. The dotted line illustrates the result of fitting the parameters of eq 4 to the data for 1 mM $CaCl_2$. The values of the parameters are $k^+ = 3.2 \pm 0.4 \times 10^4$ M^{-1} s^{-1} and $k^- = 1.0 \pm 0.8 \times 10^{-3}$ s^{-1}. Using 100 μM $CaCl_2$, the rate constants were determined to be $k^+ = 8.3 \pm 1.5 \times 10^4$ M^{-1} s^{-1} and $k^- = 4 \pm 2$ 10^{-3} s^{-1}.

Again, adsorption isotherms and concentration-dependent rate constants in the presence of 1 mM and 100 μM $CaCl_2$ were monitored. Fitting the parameters of eq 3 to the data depicted in Figure 6 leads to a maximum frequency shift of $\Delta f_{max} = -23 \pm 1$ Hz and an association constant of $K_{ass} = 2.6 \pm 0.2 \times 10^7$ M^{-1} in the presence of 1 mM $CaCl_2$. At a calcium ion concentration of 100 μM, the maximum frequency shift is significantly decreased to $\Delta f_{max} = -10 \pm 1$ Hz, while the association constant $K_{ass} = 2.6 \pm 0.4 \times 10^7$ M^{-1} is the same as that in the presence of 1 mM $CaCl_2$. This is in contrast to what was observed for lipid layers without cholesterol. While the association constant of annexin A1 binding in the absence of cholesterol decreased with decreasing calcium ion concentration in the bulk phase, it remained high in the presence of cholesterol when the calcium ion concentration decreased. In Figure 7, k_s as a function of the annexin A1 concentration in the bulk phase is plotted for 1 mM and 100 μM $CaCl_2$ in solution, respectively. By fitting the parameters of eq 4 to the data, we obtained $k^+ = 3.2 \pm 0.4 \times 10^4$ M^{-1} s^{-1} and $k^- = 1.0 \pm 0.8 \times 10^{-3}$ s^{-1} for 1 mM $CaCl_2$ and $k^+ = 8.3 \pm 1.5 \times 10^4$ M^{-1} s^{-1} and $k^- = 4 \pm 2 \times 10^{-3}$ s^{-1} for 100 μM $CaCl_2$. Similar to the results obtained for annexin A1 binding to cholesterol-free membranes, a decrease in Ca^{2+} concentration also results in a considerable increase in the rate constants of association and dissociation for cholesterol-containing membranes. In Table 1, the thermodynamic and kinetic data of annexin A1 binding to both membrane systems are summarized.

Table 1: Summary of the Thermodynamics and Kinetics Parameters Obtained for Binding of Annexin A1 to Solid-Supported Membranes Consisting of POPC/POPS (4:1) with and without 30 % Cholesterol at Different Calcium Ion Concentrations in the Bulk Phase

membrane system	POPC/POPS (4:1)		POPC/POPS/cholesterol (56:14:30)	
Ca^{2+} concentration	1 mM	100 μM	1 mM	100 μM
$-\Delta f_{max}$/Hz	21 ± 1	17 ± 2	23 ± 1	10 ± 1
$K_{ass}/10^6$ M^{-1}	17 ± 2	3.8 ± 0.7	26 ± 2	26 ± 4
$K_d/10^{-9}$ M[a]	59 ± 7	260 ± 50	39 ± 3	39 ± 6
$k^+/10^3$ M^{-1} s^{-1}	14 ± 3	53 ± 6	32 ± 4	83 ± 15
$k^-/10^{-3}$ s^{-1}	3 ± 1	7.0 ± 1.5	1.0 ± 0.8	4 ± 2

[a] K_d obtained from $1/K_{ass}$; K_d can also be calculated from the kinetics constants. As these values lead to K_d values with much larger errors, they were not listed in the table.

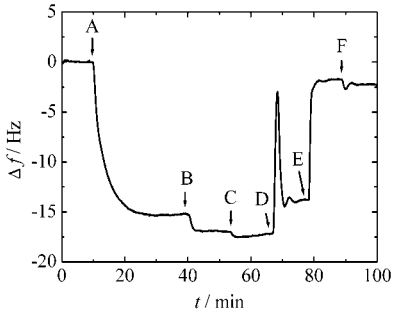

FIGURE 8: Representative time course of the adsorption of annexin A1 (A, 0.12 μM; B, 0.32 μM; C, 0.52 μM protein) to a POPC/POPS (4:1) membrane in the presence of 1 mM $CaCl_2$ followed by desorption due to stepwise complexion of Ca^{2+} by injection of EGTA solutions (D−F). The calculated free calcium ion concentrations are $1.3 \pm 0.5 \times 10^{-4}$ (D), $5.2 \pm 1.0 \times 10^{-8}$ (E), and $2.4 \pm 1.0 \times 10^{-8}$ (F) M.

Reversibility of Annexin A1 Adsorption. As annexin A1 is a cytosolic protein and most likely is recruited to the membrane following a calcium ion trigger, reversibility of calcium-induced annexin A1 binding to membranes is of crucial importance for its function. By calcium titration experiments, we intended to obtain the minimum calcium ion concentration necessary for annexin A1 binding to the lipid membranes under investigation. Moreover, the amount of irreversibly bound annexin A1 adsorbed in a calcium independent manner can be determined. A typical time course of such a calcium titration experiment is shown in Figure 8. The membrane was composed of POPC/POPS (4:1). First, annexin A1 was added to the solid-supported lipid bilayer with a concentration corresponding to maximum surface coverage (>0.4 μM) in 20 mM Tris/HCl, 0.1 M NaCl, 1 mM NaN_3, 1 mM $CaCl_2$ at pH 7.4. The decrease in resonance frequency is indicative of a successful protein binding. After equilibrium had been reached, different amounts of an EGTA-containing buffer were added to stepwise chelate the calcium ions. The addition of EGTA results in an increase in resonance frequency (Figure 8). Control experiments without bound annexin A1 ensured that the addition of EGTA did not alter significantly the resonance frequency of the quartz plate (not shown). However, it takes some time to reach equilibrium conditions after the first addition of EGTA, which is indicated by the sharp peak in Figure 8

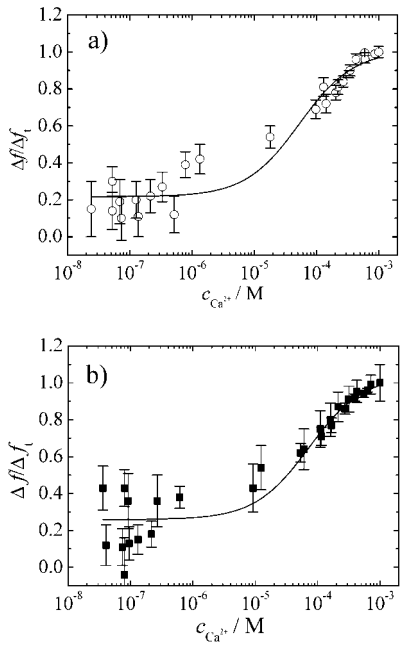

FIGURE 9: Relative increase in resonance frequency due to desorption of prebound annexin A1. (a) The membrane consisted of POPC/POPS (4:1). (b) The membrane consisted of POPC/POPS/cholesterol (56:14:30). The free calcium ion concentration was reduced by stepwise adding an EGTA-containing buffer to the solution. The point of inflection indicates the calcium ion concentration necessary for binding. The total annexin A1 concentration was >0.4 μM.

(addition E). Taking the association constants of Ca^{2+} and EGTA and the pH into account, the actual free calcium ion concentration in solution was calculated (*32*). To show the quantity of annexin A1 desorption at different free calcium ion concentrations, we defined the relative amount of bound annexin A1 as the ratio of Δf, which is defined as the actual frequency shift after EGTA addition and the total decrease in frequency shift Δf_t due to initial protein adsorption. The reversibility of binding was investigated for membranes composed of POPC/POPS (4:1) and for those containing 30 mol % cholesterol in order to explore the potential influence of cholesterol on the desorption of annexin A1. The results for both membrane systems are shown in Figure 9. The solid lines are results of fitting a Langmuir-like isotherm taking the amount of irreversibly bound protein into account. We used a Langmuir-like isotherm in order to be consistent with the previously made assumptions (see eq 3). The half-maximum calcium ion concentration necessary for annexin A1 binding to POPC/POPS (4:1) membranes was determined to be 53 $\pm$ 10 μM. A similar value of 72 $\pm$ 10 μM was obtained for annexin A1 binding to POPC/POPS/cholesterol membranes. For both membrane systems, approx. 20% of adsorbed annexin A1 remains irreversibly bound to the membrane after removing Ca^{2+}.

DISCUSSION

The interaction of annexin A1 with phospholipid vesicles and chromaffin granules and its potential of aggregating membranes have been investigated in several studies (*9*−*13*, *23*). However, kinetic parameters, which are particularly important for understanding dynamic processes such as the calcium-regulated association and dissociation of annexin A1, have so far remained elusive. Therefore, we focused in this study not only on analyzing the binding strength of full-length annexin A1 to lipid membranes at equilibrium but also on describing the binding kinetics of the reaction. Quantitative data were obtained using the quartz crystal microbalance, which has been shown to be a versatile tool to monitor protein−lipid interactions label-free and with submonolayer resolution in a time-resolved manner (*27*). By immobilizing lipid bilayers on the gold surfaces of quartz plates, it was possible to separate the event of primary and secondary binding of lipid membranes to annexin A1, which is not achievable in vesicle assays.

By fitting a Langmuir adsorption isotherm to the data, we obtained association constants and maximum surface coverage for a given calcium ion concentration and lipid composition. The application of a simple Langmuir adsorption isotherm is justified since it is known that annexin A1 binds to phosphatidylserine as a monolayer (*22*, *38*). The results indicate that annexin A1 binding was only detected if POPS and calcium ions were present, consistent with results of previous assays (*2*, *20*). Moreover, they validate the QCM technique together with solid-supported membranes as a powerful method to obtain thermodynamic and kinetic data of annexin A1 adsorption.

The amount of maximum bound annexin is similar for both membrane systems in the presence of 1 mM $CaCl_2$, though the overall POPS concentration is lower for the cholesterol containing membranes. However, a significant decrease in maximum frequency shift was observed in the POPC/POPS/cholesterol system when the Ca^{2+} concentration is decreased, revealing that the number of actual binding sites is reduced at the membrane interface.

The association constants obtained for annexin A1 binding to POPC/POPS membranes indicate that the binding affinity of annexin A1 decreases considerably with decreasing calcium ion concentration. However, the addition of cholesterol to the POPC/POPS membrane system eradicates this difference in binding affinity. Membrane binding of annexins is generally believed to take place through the formation of an annexin−Ca^{2+}−phospholipid complex in which the Ca^{2+}-binding sites are directly involved (*2*, *20*). While the binding constants of Ca^{2+} to annexin A1 in the absence of lipids are in the millimolar range (*39*, *40*), half-maximum binding of annexin A1 to phospholipid vesicles was determined to occur in the range of 10−90 micromolar Ca^{2+} (*2*, *20*, *24*−*26*).

Collectively, there is strong evidence for the involvement of cholesterol-rich microdomains in the Ca^{2+}-dependent binding of annexins to membranes (*41*). In particular, annexins A2 and A6 are present in a cholesterol- and sphingomyelin-rich membrane fraction after stimulation of smooth muscle cells (*42*, *43*), annexin A13b is associated with cholesterol-rich domains in MDCK cells (*44*), and annexins A2 and A7 are found in detergent-insoluble membrane fractions isolated from a number of cells (*45*−*47*). In another study, Ayala-Sanmartin et al. (*48*) calculated that one annexin A2 binds to 17 PS molecules. Taking these observations into account, it is conceivable that Ca^{2+}-dependent annexin A1 binding to phosphatidylserine requires the accumulation of several PS molecules, namely, a PS-enriched domain to bind with high affinity to the membrane. It is established that PS forms a 2:1 complex with Ca^{2+} and that calcium ions bind with high affinity to negatively charged PS, while Ca^{2+}-binding to zwitterionic membranes

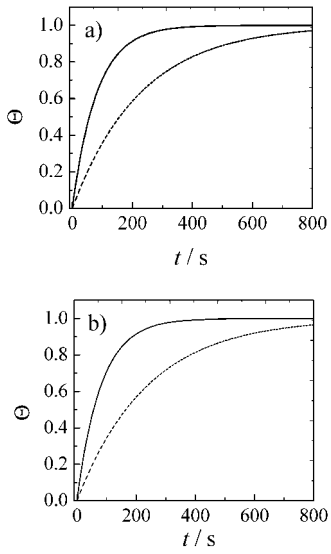

FIGURE 10: Simulated time courses of annexin A1 binding to (a) POPC/POPS membranes and (b) POPC/POPS/cholesterol membranes taking the obtained rate constants into account. The dotted lines represent the time courses in the presence of 1 mM $CaCl_2$ and the solid lines those in the presence of 100 μM $CaCl_2$. An annexin A1 concentration of 0.1 μM was assumed.

appears to be weak (*49*). This is due to the fact that the calcium ion concentration is increased near negatively charged surfaces, which can be explained by the Gouy−Chapman theory of electric double layers (*50*, *51*). Hence, an increase in Ca^{2+} concentration might favor the accumulation of PS lipids. The Ca^{2+}-induced formation of PS-enriched domains is well described for PC/PS mixture with the lipids being in the gel states (*52*). For fluid PC/PS lipids, complete miscibility is assumed. However, domains in the nanometer regime cannot be resolved by common techniques such as fluorescence microscopy. The formation of PS-enriched domains as high affinity binding sites for annexin A1 explains the result that the binding affinity of annexin A1 is not influenced by the calcium ion concentration when associated to lipid membranes composed of POPC/POPC/cholesterol. It was shown that cholesterol associates preferentially with PC and not with PS (*53*, *54*). Thus, the exclusion of PS in PC/PS/cholesterol membranes might induce the formation of PS-rich domains. This results in membranes containing PS-enriched domains, independent of the Ca^{2+} concentration, explaining that the binding constants of annexin A1 to POPS/POPS/cholesterol are not influenced by the Ca^{2+} concentration.

By means of the quartz crystal microbalance, we were, for the first time, able to obtain kinetic data on the binding of annexin A1 to lipid membranes. Rate constants of association and dissociation were obtained for POPC/POPS and POPC/POPS/cholesterol bilayers. It turned out that cholesterol does not alter the kinetic constants considerably. However, a decrease in the calcium ion concentration from 1 mM to 100 μM significantly increased both rate constants k^+ and k^-. This might be due to more conformational freedom of the protein at lower calcium ion concentrations resulting in a lower activation energy of adsorption and desorption. The effect of the increase in both rate constants for one particular annexin A1 concentration on the rate of adsorption is depicted in Figure 10. Within cells the annexin A1 concentration is estimated to be in the range of 0.01−0.1 μM, and the latter concentration was taken into account for calculating the time-resolved adsorption depicted in Figure 10. Under such conditions, it takes approx. 3 times longer to reach maximum surface coverage in the presence of 1 mM $CaCl_2$ than in a 100 μM $CaCl_2$ solution.

As membrane binding of annexins is generally thought to take place through the formation of an annexin−Ca^{2+}−phospholipid complex, protein adsorption can be analyzed by varying the annexin or the calcium ion concentration in solution. For annexin A1, its binding to and its capability of aggregating vesicles was investigated as a function of the calcium ion concentration in solution by determining the Ca^{2+} concentration ($[Ca]_{1/2}$) required for half-maximal binding to phospholipid vesicles or cell membranes. In the case of pure phosphatidylserine vesicles, this calcium ion concentration $[Ca]_{1/2}$ is in the range of 1−30 μM (*2*). Recently, Bitto and Cho determined the Ca^{2+} concentration required for half-maximal binding to be 48 μM for POPS/POPE/POPC (2:5:2) vesicles (*20*). The values obtained in our study by means of the quartz crystal microbalance technique are also in the 10 μM range. They were obtained by removing already bound annexin A1 from the membrane by titrating the Ca^{2+} concentration with EGTA in solution. The point of deflection determines the required half-maximum Ca^{2+} concentration, which was 53 μM for POPC/POPS membranes and 72 μM for POPC/POPS/cholesterol membranes, respectively. From the titration curves, it is also evident that there remains a portion of irreversibly bound annexin A1 on the surface after removing $CaCl_2$ independent of the cholesterol content in the membrane. Most likely, irreversibly bound annexins are located within defects in the lipid bilayer on the solid support due to nonspecific hydrophobic interactions, as was observed by scanning force microscopy images of lipid bilayers immobilized on mica (*38*). In addition to these calcium ion regulated interactions, it is reported that annexin A1 is also able to bind to phospholipid membranes in the absence of Ca^{2+} at low pH (*55*). However, presently the mode of this interaction is not understood, and further experiments need to be performed to address this interaction and its possible function.

CONCLUSIONS

The quartz crystal microbalance (QCM) technique, in combination with solid-supported lipid bilayers, enabled us to monitor the interaction of annexin A1 with lipid membranes without labeling the protein component and without interference from membrane aggregation. The affinity constants determined for the binding of annexin A1 to lipid membranes of different compositions reveal that at low calcium ion concentration, the presence of cholesterol increases the binding affinity of annexin A1 to lipid membranes, stressing the fact that cholesterol might be important for forming a high affinity interface for the attachment of the protein. Besides thermodynamic data, kinetics of the annexin A1 interaction were obtained for the first time by utilizing the QCM technique. The kinetic data indicate that the calcium ion concentration influences the rate of protein binding to the membrane considerably. Notably, at lower Ca^{2+} concentration, protein binding to the membrane is faster than that at higher Ca^{2+} concentrations. As it is possible to separate the events of primary and secondary binding of annexin A1 to lipid membranes using

solid-supported bilayers, which is not achievable in vesicle assays, it will be interesting to study the event of secondary binding, i.e., the interaction of membrane-bound annexin A1 with a second membrane, by means of the quartz crystal microbalance.

ACKNOWLEDGMENT

We would like to thank A. Janshoff for fruitful discussions and carefully reading this manuscript and H.-J. Galla for his generous support.

REFERENCES

1. Berrdige, M. J., Bootman, M. D., and Lipp, P. (1998) *Nature 395*, 645−648.
2. Raynal, P., and Pollard, H. B. (1994) *Biochim. Biophys. Acta 1197*, 63−93.
3. Gerke, V., and Moss, S. E. (1997) *Biochim. Biophys. Acta 1357*, 129−154.
4. Gerke, V., and Moss, S. E. (2002) *Physiol. Rev. 82*, 331−371.
5. Rosengarth, A., Gerke, V., and Luecke, H. (2001) *J. Mol. Biol. 306*, 489−498.
6. Rosengarth, A., and Luecke, H. (2000) *Acta Crystallogr, Sect. D 56*, 1459−61.
7. Huber, R., Berendes, R., Burger, A., Schneider, M., Karshikov, A., and Luecke, H. (1995) *J. Mol. Biol. 223*, 683−704.
8. Luecke, H., Chang, B. T., Mailliard, W. S., Schlaepfer, D. D., and Haigler, H. T. (1995) *Nature 378*, 512−515.
9. de la Fuente, M., and Parra, V. (1995) *Biochemistry 34*, 10393−10399.
10. Meers, P., Mealy, T., Pavltsky, N., and Tauber, A. I. (1992) *Biochemistry 31*, 6372−6382.
11. Meers, P., Mealy, T., and Tauber, A. I. (1993) *Biochim. Biophys. Acta 1147*, 177−184.
12. Wang, W., and Creutz, C. E. (1992) *Biochemistry 31*, 9934−9939.
13. Wang, W., and Creutz, C. E. (1994) *Biochemistry 33*, 275−282.
14. Swairjo, M. A., Concha, N. O., Kaetzel, M. A., Deman, J. R., and Seaton, B. A. (1995) *Nat. Struct. Biol. 2*, 968−974.
15. Huber, R., Römisch, J., and Paques, E. P. (1990) *EMBO J. 9*, 3867−3874.
16. Voges, D., Berendes, R., Burger, A., Demange, P., Baumeister, W., and Huber, R. (1994) *J. Mol. Biol. 238*, 199−213.
17. Jost, M., Thiel, C., Weber, K., and Gerke, V. (1992) *Eur. J. Biochem. 207*, 923−930.
18. Jost, M., Weber, K., and Gerke, V. (1994) *Biochem. J. 298*, 923−930.
19. Nelson, M. R., and Creutz, C. E. (1995) *Biochemistry 34*, 3121−3132.
20. Bitto, E., and Cho, W. (1998) *Biochemistry 37*, 10231−10237.
21. Bitto, E., and Cho, W. (1999) *Biochemistry 38*, 14094−14100.
22. Bitto, E., Li, M., Tikhonov, A. M., Schlossman, M. L., and Cho, W. (2000) *Biochemistry 39*, 13469−13477.
23. de la Fuente, M., and Ossa, C. G. (1997) *Biophys. J. 71*, 383−387.
24. Schlaepfer, D. D., and Haigler, H. T. (1986) *J. Biol. Chem. 262*, 6931−6937.
25. Ando, Y., Imamura, S., Hong, Y.-M., Owada, M. K., Kakunaga, T., and Kannagi, R. (1989) *J. Biol. Chem. 264*, 6948−6955.
26. Blackwood, R. A., and Ernst, J. D. (1990) *Biochem. J. 266*, 195−200.
27. Janshoff, A., Galla, H.-J., and Steinem, C. (2000) *Angew. Chem., Int. Ed. Engl. 39*, 4004−4032.
28. Janshoff, A., and Steinem, C. (2001) in *Sensors Update* (Baltes, H., Hesse, J., and Korvink, J. G., Eds.) pp 313−354, Wiley-VCH, Weinheim, Germany.
29. Eing, A., Janshoff, A., Galla, H.-J., and Steinem, C. (2002) *ChemBioChem 3*, 190−197.
30. Rosengarth, A., Rösgen, J., Hinz, H.-J., and Gerke, V. (1999) *J. Mol. Biol. 288*, 1013−1025.
31. Plant, A. L. (1993) *Langmuir 9*, 2764−2767.
32. Stockbridge, N. (1987) *Comput. Biol. Med. 17*, 299−304.
33. Janshoff, A., Steinem, C., Sieber, M., and Galla, H.-J. (1996) *Eur. Biophys. J. 25*, 105−113.
34. Janshoff, A., Steinem, C., Sieber, M., el Baya, A., Schmidt, M. A., and Galla, H.-J. (1997) *Eur. Biophys. J. 26*, 261−270.
35. Steinem, C., Janshoff, A., Wegener, J., Ulrich, W.-P., Willenbrink, W., Sieber, M., and Galla, H.-J. (1997) *Biosens. Bioelectron. 12*, 787−808.
36. Ulman, A. (1996) *Chem. Rev. 96*, 1533−1554.
37. Sauerbrey, G. (1959) *Z. Phys. 155*, 206−222.
38. Janshoff, A., Ross, M., Gerke, V., and Steinem, C. (2001) *ChemBioChem 7/8*, 587−590.
39. Rosengarth, A., Rösgen, J., Hinz, H.-J., and Gerke, V. (2001) *J. Mol. Biol. 306*, 825−835.
40. Rösgen, J., and Hinz, H.-J. (2001) *J. Mol. Biol. 306*, 809−824.
41. Ayala-Sanmartin, J. (2001) *Biochem. Biophys. Res. Com. 283*, 72−79.
42. Babiychuk, E. B., and Draeger, A. (2000) *J. Cell Biol. 150*, 1113−1124.
43. Babiychuk, E. B., Palstra, R. J., Schaller, J., Kampfer, U., and Draeger, A. (1999) *J. Biol. Chem. 274*, 35191−35195.
44. Lafont, F., Lecat, S., Verkade, P., and Simons, K. (1998) *J. Cell Biol. 142*, 1413−1427.
45. Clemen, C. S., Hofmann, A., Zamparelli, C., and Noegel, A. A. (1999) *J. Muscle Res. Cell Motil. 20*, 669−679.
46. Sagot, I., Regnouf, F., Henry, J.-P., and Pradel, L.-A. (1997) *FEBS Lett. 410*, 229−234.
47. Oliferenko, S., Satha, K., Harder, T., Gerke, V., Schwarzler, C., Schwarz, H., Beug, H., Gunthert, U., and Huber, L. A. (1999) *J. Cell Biol. 146*, 843−854.
48. Ayala-Sanmartin, J., Henry, J.-P., and Pradel, L.-A. (2001) *Biochim. Biophys. Acta 1510*, 18−28.
49. Huster, D., Arnold, K., and Gawrisch, K. (2000) *Biophys. J. 78*, 3011−3018.
50. McLaughlin, S., Mulrine, N., Gresalfi, G., Vaio, G., and McLaughlin, A. (1981) *J. Gen. Physiol. 77*, 445−473.
51. McLaughlin, S. (1977) *Curr. Top. Membr. Transp. 9*, 71−144.
52. Ross, M., Steinem, C., Galla, H.-J., and Janshoff, A. (2001) *Langmuir 17*, 2437−2445.
53. Bach, D., Borochov, N., and Wachtel, E. (1998) *Chem. Phys. Lipids 92*, 71−77.
54. Yeagle, P. L., and Young, J. E. (1986) *J. Biol. Chem. 261*, 8175−8181.
55. Rosengarth, A., Wintergalen, A., Galla, H.-J., Hinz, H.-J., and Gerke, V. (1998) *FEBS Lett. 438*, 279−284.

BI025951Z